J|A|C|S ARTICLES

Published on Web 10/19/2010

Elementary Building Blocks of Self-Assembled Peptide Nanotubes

Nadav Amdursky,[†] Michel Molotskii,[‡] Ehud Gazit,[†] and Gil Rosenman*[,‡]

Department of Molecular Microbiology and Biotechnology, George S. Wise Faculty of Life Sciences, and School of Electrical Engineering, Iby and Aladar Fleischman Faculty of Engineering, Tel Aviv University, Tel Aviv 69978, Israel

Received May 20, 2010; E-mail: gilr@eng.tau.ac.il

Abstract: In the world of biology, "self-assembly" is the ability of biological entities to interact with one another to form supramolecular structures. One basic group of self-assembled structures is peptide nanotubes (PNTs). However, the self-assembly mechanism, with its special characteristics, is not yet fully understood. An exceptional quantum-confined approach is shown here for the self-assembly mechanism in bio-inspired materials. We found the elementary building block of the studied PNT, which is self-assembled from short peptides composed of two phenylalanine residues, to be 0D-quantum-confined (can be related to confinement in 3D), also called a quantum dot (QD). This elementary building block can further self-assemble to a PNT formation. It has been observed that the assembly process of dots to tubes and the disassembly process of tubes to dots are reversible. We further show that a similar dipeptide can also self-assemble to a QD-like structure, with different dimensions. The presented peptide QD structures are nanometer-sized structures, with pronounced exciton effects, which may promote the use of an entirely new kind of organic QDs.

Introduction

Bio-inspired structures can be composed from biological, organic, and inorganic materials. They possess unique properties due to their inspiration from biological entities, which were created during the long evolution process.[1,2] The use of organic materials to replace the common metallic/semiconductor materials in the micro- and nano-industries has attracted much interest during the past decade. The most common approach for the use of organic materials in this industry is their conjugation at the metallic/semiconductor−organic framework.[3,4] One of the most studied bio-organic groups in this context is that of proteins and peptides.[5−7] The chosen amino acids and length of the peptide chain can vary significantly from one peptide to another, thus creating almost unlimited possibilities for the composition of a certain peptide. Some of the proteins and peptides have the ability to self-assemble and, as a result, form a defined architecture, which does not resemble their building block architecture. This way of formation represents a bottom-up approach, which is distinct from the common top-down approach in current nanolithography and possesses unique advantages.[8] The self-assembly process of proteins and peptides involves several weak, non-covalent bonds, such as ionic, van der Waals, hydrogen bonding, hydrophobic, and π-stacking.[9] The latter has an important role in the self-assembly process of amyloid proteins,[10] which are associated with amyloid diseases (such as Alzheimer's disease (AD), Parkinson's disease, and more). The minimal core recognition motif of the amyloid-β protein, which is associated with AD, is composed from two aromatic phenylalanine residues. It has been shown that the dipeptide composed from two phenylalanine residues, diphenylalanine (FF), can self-assemble to peptide nanotubes (PNTs)[11] which possess a hexagonal crystal structure space group of $P6_1$.[12] Herein we study the self-asembly process and fine structure of two different aromatic dipeptides, NH_2-Phe-Phe-COOH (FF) and NH_3-Phe-Trp-COOH (FW), by measurements of optical absorption and luminescence effects. We recently observed the formation of nanoscale regions in PNTs and peptide nanospheres, which demonstrated pronounced quantum confinement (QC) phenomena in these structures due to specific behavior of optical and luminescence spectra. We showed a 0D-quantum-confined structure, also known as a quantum dot (QD) structure, within micrometer-size peptide spheres made from an analogue of the FF dipeptide.[13] We also found a 2D-quantum-confined structure, also known as a quantum well structure, within PNTs which were made by a special vapor deposition process.[14]

It is shown in this work that, from optical absorption and luminescence data, we can conclude that the FF PNT is

[†] Department of Molecular Microbiology and Biotechnology.
[‡] School of Electrical Engineering.

(1) Pfeifer, R.; Lungarella, M.; Iida, F. *Science* **2007**, *318*, 1088.
(2) Xia, F.; Jiang, L. *Adv. Mater.* **2008**, *20*, 2842.
(3) James, S. L. *Chem. Soc. Rev.* **2003**, *32*, 276.
(4) Bent, S. F. *Surf. Sci.* **2002**, *500*, 879.
(5) Ulijn, R. V.; Smith, A. M. *Chem. Soc. Rev.* **2008**, *37*, 664.
(6) Zhao, X. J.; Zhang, S. G. *Chem. Soc. Rev.* **2006**, *35*, 1105.
(7) Gazit, E. *Chem. Soc. Rev.* **2007**, *36*, 1263.
(8) Shimomura, M.; Sawadaishi, T. *Curr. Opin. Colloid Interface Sci.* **2001**, *6*, 11.
(9) Zhang, S. G. *Nat. Biotechnol.* **2003**, *21*, 1171.
(10) Gazit, E. *FASEB J.* **2002**, *16*, 77.
(11) Reches, M.; Gazit, E. *Science* **2003**, *300*, 625.
(12) Gorbitz, C. H. *Chem. Eur. J.* **2001**, *7*, 5153.
(13) Amdursky, N.; Molotskii, M.; Gazit, E.; Rosenman, G. *App. Phys. Lett.* **2009**, *94*, 261907.
(14) Amdursky, N.; Molotskii, M.; Aronov, D.; Adler-Abramovich, L.; Gazit, E.; Rosenman, G. *Nano Lett.* **2009**, *9*, 3111.

 10.1021/ja104373e

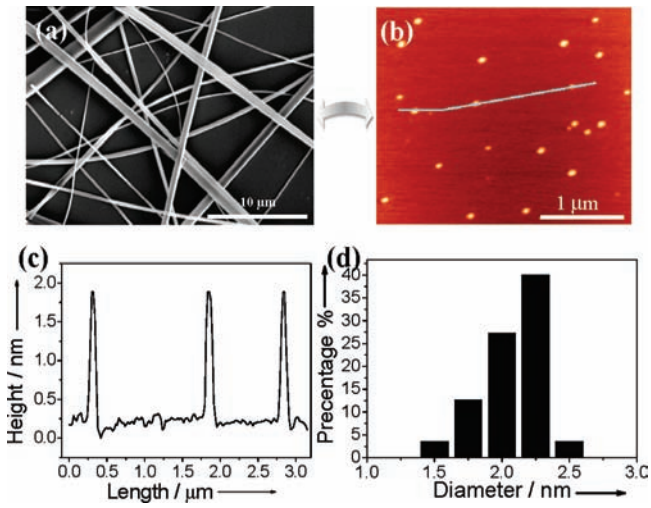

Figure 1. (a) Scanning electron microscopy image of the FF PNTs. (b) Atomic force microscopy image of the FF PQDs. The double arrow between (a) and (b) symbolizes the reversibility of the process, from PQD to PNT and vice versa. (c) A cross section along the blue line at (b), which shows the height of the PQD. (d) A height histogram of the FF PQD.

composed of QD-like structures. We further show that these quantum-confined regions are in fact the elementary building blocks of the PNTs, and they can also exist as a single entity in a solution. We refer to these QD-like nanostructures as peptide quantum dots (PQDs). The pronounced QC and exciton effects allow us to directly observe the self-assembly and disassembly processes of the elementary building blocks of the PNTs.

Results and Discussion

The first stage of forming either the dot structure or the PNT structure from the FF peptide monomer is to dissolve the FF powder in a strong solvent of hexafluoro-2-propanol (HFIP), which allows the FF monomers to stay in their monomeric state and not form any structure. For forming the PQD structure, the concentrated HFIP solution was dissolved in methanol at a desired concentration (2−10 mg/mL). For forming the PNT structure, the concentrated HFIP solution was dissolved in ddH_2O at a desired concentration (2−5 mg/mL). It is important to stress that, at low concentration (<1 mg/mL), the FF monomers tend to stay in their monomeric state and not form PQD or tube structure. Figure 1 shows images of the FF PNTs (Figure 1a) and PQDs (Figure 1b). The PQDs have a homogeneous diameter, as can be seen in the cross section (Figure 1c). The size distribution of the FF PQDs was measured (Figure 1d). The size distribution displays an average diameter of 2.12 ± 0.15 nm for the PQDs. In contrast, the PNTs (Figure 1a) have a wide diversity in their diameter, which can range from 50 nm to several micrometers. When the methanol environment of the PQDs is changed to aqueous solution, the PQDs undergo a further self-assembly process to the PNT structure. We found that this process is reversible; thus, we can dilute the PNTs in methanol again to restore the PQD structure. The reversibility of the process is due to the crucial effect of water molecules in the assembly of PNT structure. The nanotubes are formed via a network of hydrogen bonds between the backbone of the peptide and water molecules, which can enter the hydrophilic channels of the nanotube layer.[15] As a consequence, in aqueous solution water can sustain the network of hydrogen bonds, and

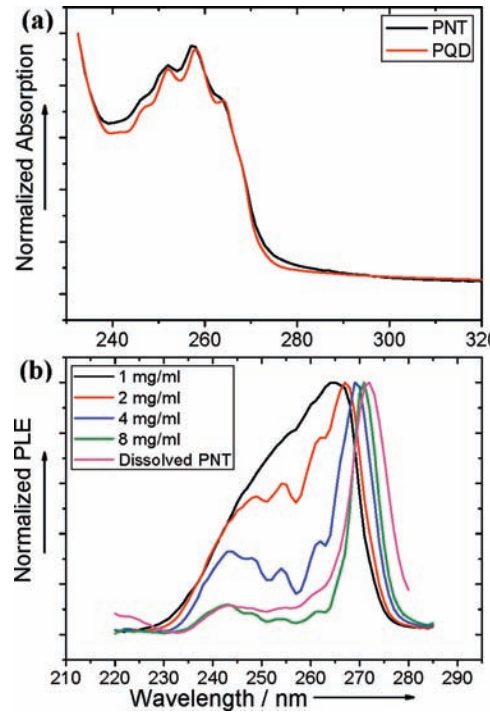

Figure 2. (a) Optical absorption spectrum of the FF PNTs (black line) and the FF PQDs (red curve). (b) PLE spectrum of the FF PQDs at several concentrations, along with the PLE spectrum of a dissolved FF PNT in methanol. The emission wavelength is 290 nm.

the PQD will self-assemble into PNT structure, whereas in a methanol environment the network of hydrogen bonds cannot be supported, but the strong aromatic interactions that form the crystalline structure of the PQD are not interrupted. As a consequence, the PNT will disassemble into its elementary building blocks of PQD and not to its FF monomers. We will show that the structures within the organic solution possess a unique signature that allows us to ascribe the structures to PQD and not simply FF monomers.

For ascribing the formed nanoparticle and nanotube structures to be a QC structure composed of nanosize particles which behave as QDs, spectroscopic measurements were used. The optical absorption properties are defined by the electron/hole energy spectrum, and the optical absorption coefficient is proportional to the density of electronic states (DOS) of the material. Different QC structures have completely different DOS behaviors, in which QD structure possesses spike-like behavior.[16]

The optical absorptions of both the PQDs and PNTs possess identical spike-like behavior (Figure 2a), which is evidence for the existence of identical nanosize regions of QDs in both of the structures. The most distinguishing feature of QC structures is a strong Coulomb interaction between electrons and holes due to high confinement of electron and holes in the QD structure, which leads to the formation of an exciton. Thus, we can follow the formation of the exciton, and consequently observe the QC structure, by measuring the exciton luminescence. Figure 2b shows the photoluminescence excitation (PLE) spectrum of the PQDs at several concentrations. We can clearly observe the formation of the exciton by the narrow excitation peak (full width at half-maximum (fwhm) of 6 nm) at 270 nm at high concentrations. High concentration is distinguished by

(15) Görbitz, C. H. *Chem. Commun.* **2006**, 2332.

(16) Svelto, O. *Principles of Lasers*; Pleneum Press: New York, 1998.

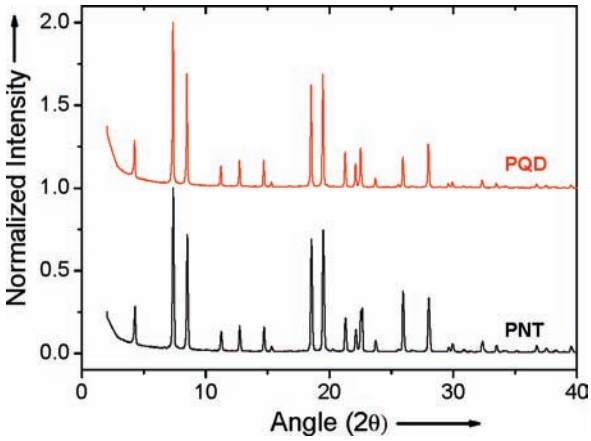

Figure 3. XRD spectrum of the FF PNTs (black curve) and the FF PQDs (red curve).

the formation of the PQDs, whereas low concentration is distinguished by the presence of free monomers. The PLE curve of the low-concentration sample is broad and does not show the sharp exciton peak. The formation of the narrow peak is direct evidence of the formation of crystalline structure in the PQDs.[17,18] As in common QC systems, the exciton peak is located at the red edge of the absorption spectrum.[19] As in our previously work on QDs within large peptide spheres,[13] we observe a known effect of a phononless exciton line and its phonon replicas (further discussion is given in the Supporting Information).

For further validation that PQDs are the elementary building blocks of the FF PNTs, X-ray diffraction (XRD) patterns were used. Figure 3 shows the XRD of the FF PQDs and PNTs. It can be clearly seen that both of the structures possess the same crystal structure, which correlates to the $P6_1$ space group (the fit of the XRD pattern to the $P6_1$ space group is shown in Figure S1 in the Supporting Information).

From the optical absorption and PLE spectra, we can calculate the dimensions of the confined structure by using our theoretical model of organic QD.[13] In this model we define the radius of a QD as

$$R = \pi r_B^0 \sqrt{\frac{m_0/M}{\frac{\mu}{m_0\varepsilon_\infty^2} - \frac{E_{ex}^{QD}}{Ry}}} \quad (1)$$

where $r_B^0 = \hbar^2/m_0e^2 = 0.53$ Å is the Bohr radius of the hydrogen atom, m_0 is the free electron mass, $Ry = m_0e^4/2\hbar^2 = 13.56$ eV is the Rydberg constant, $M = m_e + m_h$ is the translation mass of the exciton (m_e and m_h are the effective mass of electron and hole, respectively), $\mu = m_em_h/(m_e + m_h)$ is the reduced exciton mass, ε_∞ is the high-frequency dielectric constant of the QD, and E_{ex}^{QD} is the exciton binding energy. Due to the lack of known electronic properties of FF PQDs, we have used the refractive index of the similar benzene crystal, with $n = 1.5$,[20] for calculating ε_∞. This defines ε_∞ as $\varepsilon_\infty = n^2 = 2.25$. The optical absorption and PLE bands start from $\lambda_{ion} = 242$ nm ($\hbar\omega_{ion} = 5.12$ eV), which is the breaking of the binding exciton state. The value of $\hbar\omega_{ion}$ corresponds to the energy gap of the QD, which corresponds to the value of the transport gap of a similar crystal, such as benzenethiol, ~5.1 eV.[21,22] The difference between $\hbar\omega_{ion}$ and the phononless line $\hbar\omega_g^0 = 4.59$ eV is equal to 0.53 eV. This energy represents the exciton binding energy, E_{ex}^{QD}, of the QD. The effective masses of electrons and holes are almost equal and close to $0.5m_0$.[23] Consequently, for $\mu = 1/2m_e = 0.25m_0$ and $M = m_0$, we obtain from eq 1 a value of the PQD radius as $R \approx 1.65$ nm.

The size of the PQDs, which was measured both by microscopy (Figure 1b,c) and by theoretical calculation, suggests that each PQD is composed of two FF monomers. Reinforcement for this argument can be seen in the single-crystal model of the FF PNTs made by Görbitz.[15] This model suggests a representation for the inner surface of the nanotubes, containing multiple hydrophilic/hydrophobic channels, aligned parallel to the main axis of the tube (Figure 3 of ref 15). This model presents a grain-shaped structure within the PNTs. The boundaries of the grains are two adjacent channels, with an approximate size between the channels of ~2 nm, where the radius of the aromatic area is around 1.5 nm. Each grain in this model is composed of two FF monomers. We suggest that the QC crystal structure is formed due to the aromatic rings of the phenylalanine residues. This model fits both to our calculation of the radius of the confined crystal structure and to the size of the PQD composed of two FF molecules.

To confirm our assumption about the composition of the PQD structure, time-of-flight secondary ion mass spectrometry (ToF-SIMS) and mass spectrometry (MS) measurements were performed (Figure 4a and b, respectively). In both the ToF-SIMS and MS measurements, we found a peak that corresponds to the molecular weight of two phenylalanine residues (623 g/mol). The ToF-SIMS analysis (Figure 4a) shows a single peak at 623 *m*/*z* (mass-to-charge ratio). The MS analysis (Figure 4b) shows a slightly higher value for the molecular mass of the PQD, due to the involvement of sodium ions in the process. The peaks in the MS measurement correspond to two FF molecules with two or three sodium ions, 669.3 and 691.3 *m*/*z*, respectively.

In order to check whether the formation of nanosize PQD particles with pronounced exciton effects, and their further self-assembly to PNTs, is unique to the FF molecule or can be ascribed to other peptides, we decided to check another small dipeptide. The chosen dipeptide of FW is similar to the FF peptide, due to its high aromaticity level. FW has a spectroscopic signature similar to that of the FF peptide (Figure 5a). Its optical absorption spectrum also consists of several peaks (blue curve), though the peaks here are broader in comparison to the absorption peaks of the FF peptide (Figure 2a), which might be the result of disorder in the nanocrystalline structure.[24] The PLE characteristics also exhibit similar behavior to those of the FF peptide. Whereas the low-concentration sample of 0.125 mg/mL displays a broad PLE spectrum (Figure 4a, black curve), the high-concentration sample of 2 mg/mL displays a narrow

(17) Nelson, R. J. *Excitons*; North-Holland: Amsterdam, 1982.
(18) Schubert, E. F.; Gobel, E. O.; Horikoshi, Y.; Ploog, K.; Queisser, H. J. *Phys. Rev. B* **1984**, *30*, 813.
(19) Muth, J. F.; Lee, J. H.; Shmagin, I. K.; Kolbas, R. M.; Casey, H. C.; Keller, B. P.; Mishra, U. K.; DenBaars, S. P. *Appl. Phys. Lett.* **1997**, *71*, 2572.
(20) Kaye, G. W.; Laby, T. H. *Tables of Physical and Chemical Constants*; Longmans, Green & Co.: London, 1959.
(21) Lalov, I. J.; Zhelyazkov, I. *Phys. Rev. B* **2007**, *75*.
(22) Zangmeister, C. D.; Robey, S. W.; van Zee, R. D.; Yao, Y.; Tour, J. M. *J. Phys. Chem. B* **2004**, *108*, 16187.
(23) Sanchez-Carrera, R. S.; Coropceanu, V.; Kim, E. G.; Bredas, J. L. *Chem. Mater.* **2008**, *20*, 5832.
(24) Talgorn, E.; Moysidou, E.; Abellon, R. D.; Savenije, T. J.; Goossens, A.; Houtepen, A. J.; Siebbeles, L. D. A. *J. Phys. Chem. C* , *114*, 3441.

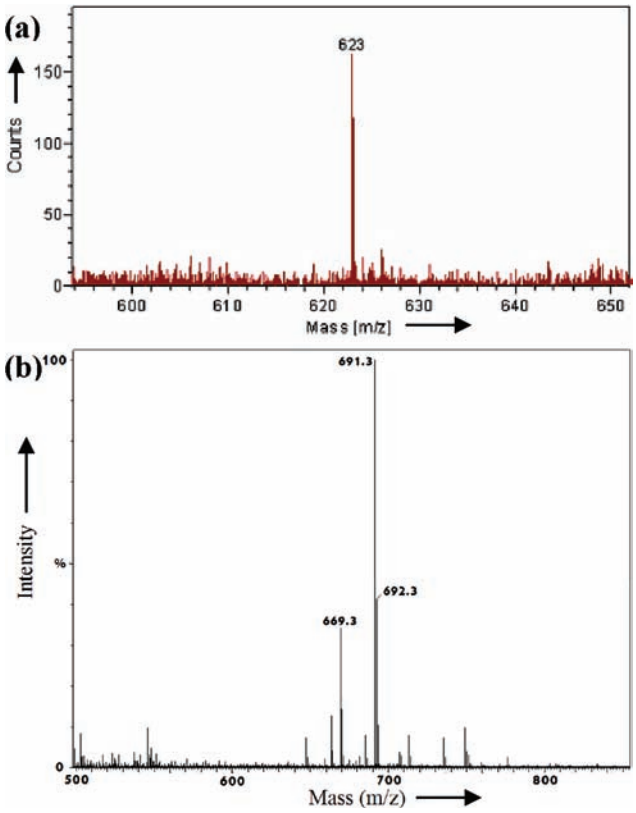

Figure 4. (a) ToF-SIMS and (b) MS analysis of the FF PQDs. Both of the analyses show the FF PQD composition from two FF molecules.

PLE spectrum (red curve), with a fwhm of 12 nm, which indicates the formation of an exciton. Similar to the absorption peaks, the fwhm of the FW peptide is also broader than the fwhm of the FF peptide (6 nm). The spectroscopic analysis of FW suggests that FW can also undergo self-assembly to the PQD structure. By using eq 1, we can calculate the expected dimensions of the PQD. In the FW PQD structure, the exciton peak is located at 306 nm (4.05 eV). The optical absorption bands start from $\lambda_{ion} = 293$ nm ($\hbar\omega_{ion} = 4.23$ eV). As explained above, we can find from these two values the exciton binding energy to be $E_{ex}^{QD} = 185$ meV. From eq 1, the FW PQD radius is $R \approx 9$ Å.

To validate our calculations, we measured the formed PQD structure by AFM (Figure 5b). Unlike the FF PQDs, we could not achieve single FW PQD structures. The FW PQDs tend to aggregate, forming a single layer on the surface. The inset of Figure 5b shows a cross section along the green line, which points to a height of 1.1−1.3 nm. This height is lower than the height of the FF PQD (~2.1 nm) and close to the calculated value of 9 Å.

It is important to notice that, in contrast to the FF peptide, the FW peptide does not form PNTs in aqueous solution, which remains transparent, unlike the turbid solution of the FF PNTs. The spectroscopic characteristics (Figure 5a), which point to the formation of PQDs, can be achieved in both ddH_2O and organic solvent (such as methanol).

There are several synthesis methods to produce conventional semiconductor-based QDs;[25] the most common techniques involve molecular beam epitaxy,[26] organometallic chemical vapor deposition,[27,28] colloidal chemical synthesis,[29] or an

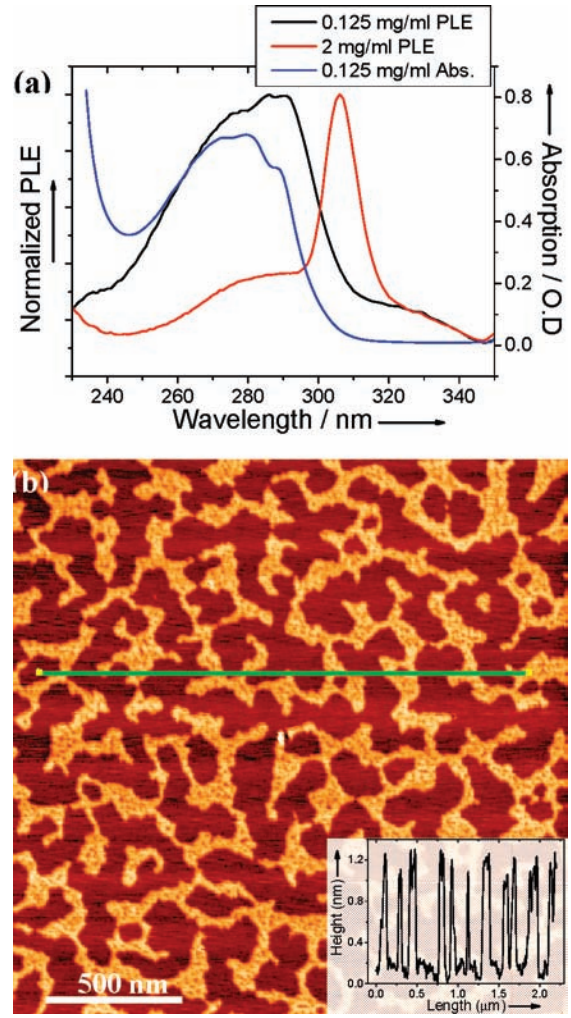

Figure 5. (a) Optical absorption (blue curve) and PLE (black and red curves) spectra of FW PQD. The emission wavelength is 365 nm. (b) AFM image of the FW PQD layer. The inset shows a cross section along the green line.

electron beam.[30] All of the described synthesis methods can yield a narrow size distribution of the QDs, ranging from single nanometers to dozens of nanometers. However, due to the process of synthesizing semiconductor QDs, producing one-size, homogeneous QDs can be difficult. On the other hand, the forces that are involved in the formation of the PQDs are non-covalent, mainly the aromatic interaction between the aromatic rings of the phenylalanine. In this manner, the size of the PQDs is determined by an energetic process, where the final structure represents the minimal energetic structure. This formation process has both advantages and disadvantages. This process is theoretically supposed to yield a one-size distribution of PQDs. This advantage is also a disadvantage, in that we cannot tune the size of the PQDs, in contrast to the conventional

(25) Alivisatos, A. P. *Science* **1996**, *271*, 933.
(26) Xin, S. H.; Wang, P. D.; Yin, A.; Kim, C.; Dobrowolska, M.; Merz, J. L.; Furdyna, J. K. *Appl. Phys. Lett.* **1996**, *69*, 3884.
(27) Dabbousi, B. O.; RodriguezViejo, J.; Mikulec, F. V.; Heine, J. R.; Mattoussi, H.; Ober, R.; Jensen, K. F.; Bawendi, M. G. *J. Phys. Chem. B* **1997**, *101*, 9463.
(28) Danek, M.; Jensen, K. F.; Murray, C. B.; Bawendi, M. G. *Chem. Mater.* **1996**, *8*, 173.
(29) Guzelian, A. A.; Banin, U.; Kadavanich, A. V.; Peng, X.; Alivisatos, A. P. *Appl. Phys. Lett.* **1996**, *69*, 1432.
(30) Ishikawa, T.; Nishimura, T.; Kohmoto, S.; Asakawa, K. *Appl. Phys. Lett.* **2000**, *76*, 167.

semiconductor QD structure. However, by using different peptides, such as the described FW peptide, we can tune the size of the PQDs. By modifying the peptide chain, we were able to change the size of the PQDs. The variety of 20 natural amino acids and the non-conventional amino acids, plus the ability to change the length of the peptide chain, can lead to endless combinatorial options for small peptides, which can result in further tuning of the PQD structures. Another advantage the PQDs possess, in comparison with conventional QDs, is their unsophisticated, fast, and cheap formation process, whereas some of the described synthesis processes for conventional QDs require the use of sophisticated and expensive processes.

Conclusions

In conclusion, we followed the self-assembly process of FF PNTs by a QC approach. We showed that the FF PNTs are composed of nanocrystalline regions, which behave as QDs, and can be referred to as the elementary building block of the nanotube. This self-assembly process, from PQDs to PNTs, can be reversible, depending on the solution environment of the structure. In this way we introduce both the bottom-up approach for the formation of the PNTs and the top-down approach for the disassembly of the PNTs to PQDs. We further showed that a similar dipeptide, FW, can also self-assemble into PQD nanoparticles but with a different radius. The self-assembled nanoscale structures, which possesses QC features, have exceptional electronic and photonic properties, which make them new candidates for luminescence devices.[31−34] In this context, the FF PNTs and PQDs show exciton formation and luminescence at room temperature; thus, their integration in luminescence devices can be promising. Both the PNTs and PQDs have technological advantages due to the morphological difference between them. In some cases, the dot morphology is preferred,[32,33] whereas in other cases the tube formation is favored.[31,34] We show here the simplicity of changing the peptide architecture.

Experimental Section

PNT Preparation. PNTs were prepared by dissolving the lyophilized form of the FF/FW building blocks in 1,1,1,3,3,3-hexafluoro-2-propanol (HFIP) at a concentration of 100 mg/mL. The FF stock solution was diluted to a final concentration of 2 mg/mL in ddH_2O for the nanotubes' self-assembly process to occur. To avoid any pre-aggregation and assembly, fresh stock solutions were prepared for each experiment.

PQD Preparation. FF PQDs were prepared in two ways. The first was to dissolve the prepared PNTs in a methanol solution. The second was to dilute the stock solution (FF in HFIP) in methanol at different concentrations, 1−8 mg/mL. FW PQDs were prepared by dissolving the FW stock solution in either ddH_2O or methanol.

Instrumental Details. XRD Analysis. XRD patterns were recorded using a symmetric Bragg geometry Scintag powder diffractometer equipped with Cu Kα radiation source and a liquid-nitrogen-cooled Ge solid-state detector.

ToF-SIMS Analysis. ToF-SIMS analysis was carried out using a Physical Electronics TRIFT II ToF-SIMS instrument with a 15 kV Ga primary ion gun.

MS Analysis. MS data were collected on a Waters SYNAPT MS system in electrospray positive ion mode.

Scanning Electron Microscopy Measurements. The samples were coated with palladium−gold and scanned using a JSM JEOL 6300 scanning electron microscope operating at 5−10 kV.

Atomic Force Microscopy Measurements. AFM analysis was done by depositing an aliquot of FF PQD on a freshly cleaved mica surface. The samples were probed by a Digital Instrument (DI) MultiModeTM NanoScope IV AFM using a Mikromasch NSC15/Si3N4 cantilever (resonant frequency $f = 325$ kHz, spring constant $k = 40$ N/m) in a tapping mode.

Optical Measurements. The optical absorption measurements were performed using a Cary 5000 UV−vis−NIR spectrophotometer (Varian, a part of Agilent Technologies, USA). The PL and PLE measurements were performed using a FluoroMax-3 spectrofluorometer (Horiba Jobin Yvon, USA).

Acknowledgment. We thank Prof. D. Huppert for helpful discussions and for assistance with the photoluminescence measurements, Y. Rosenberg for the XRD measurement, N. Tal for providing the MS measurements, and A. Daikich for the ToF-SIMS analysis. N.A. and E.G. acknowledge support from the Israel Science Foundation.

Supporting Information Available: Fitting of the XRD patterns to the $P6_1$ space group; discussion on the phononless exciton line and its phonon replica. This material is available free of charge via the Internet at http://pubs.acs.org.

JA104373E

(31) Li, Y.; Qian, F.; Xiang, J.; Lieber, C. M. *Mater. Today* **2006**, *9*, 18.
(32) Bhattacharya, P.; Ghosh, S.; Stiff-Roberts, A. D. *Annu. Rev. Mater. Res.* **2004**, *34*, 1.
(33) Narukawa, Y.; Kawakami, Y.; Funato, M.; Fujita, S.; Fujita, S.; Nakamura, S. *Appl. Phys. Lett.* **1997**, *70*, 981.
(34) Qian, F.; Li, Y.; Gradecak, S.; Park, H. G.; Dong, Y. J.; Ding, Y.; Wang, Z. L.; Lieber, C. M. *Nat. Mater.* **2008**, *7*, 701.